Catal Lett (2008) 123:307–316
DOI 10.1007/s10562-008-9424-6

Phosgene-Free Synthesis of Phenyl Isocyanate by Catalytic Decomposition of Methyl *N*-Phenyl Carbamate over Bi_2O_3 Catalyst

Yunsheng Dai · Yue Wang · Jie Yao · Qingyin Wang · Liangming Liu · Wei Chu · Gongying Wang

Received: 13 December 2007 / Accepted: 26 January 2008 / Published online: 20 February 2008

Abstract A phosgene-free approach for the synthesis of phenyl isocyanate (PI) was developed, using the heterogeneous catalytic decomposition of methyl *N*-phenyl carbamate (MPC). Twenty oxide-catalysts were investigated and compared; the Bi_2O_3 catalyst gave the better catalytic performance. From bismuth (III) nitrate pentahydrate, Bi_2O_3 was prepared by different methods, which included the direct decomposition, mechano-chemical method, direct precipitation and indirect precipitation. The catalysts were characterized by N_2 adsorption/desorption, XRD, FTIR and TEM analyses. After optimization, the Bi_2O_3 catalyst prepared by direct calcination of bismuth (III) nitrate pentahydrate at 723 K in air for 4 h gives the best activity. When the reaction was carried out at the boiling temperature of *o*-dichlorobenzene (ODCB) at normal pressure, the optimal reaction conditions over Bi_2O_3 catalyst are as follows: the mass ratio of catalyst/MPC is 0.05, mass ratio of ODCB/MPC is 15:1, reaction time of 60 min. The optimized conversion of MPC and the yield of PI are 86.2% and 78.5%, respectively. There was a good durability for the Bi_2O_3 catalyst, and the species of Bi (III) ions of catalyst were partially oxidized to Bi (IV) ions during the reaction, supported by the results of XRD and XPS techniques.

Y. Dai · Y. Wang · J. Yao · Q. Wang · L. Liu · G. Wang (✉)
Chengdu Institute of Organic Chemistry, Chinese Academy of Sciences, Chengdu 610041, China
e-mail: gywang@cioc.ac.cn

Y. Dai
Graduate School of the Chinese Academy of Sciences, Beijing 100039, China

W. Chu
Department of Chemical Engineering, Sichuan University, Chengdu 610065, China

Keywords Phosgene-free synthesis · Isocyanate · Methyl *N*-phenyl carbamate · Bismuth oxide · Dimethyl carbonate

1 Introduction

Phenyl isocyanate (PI), as a highly reactive aromatic monoisocyanate, is an important intermediate for the synthesis of pesticide and medicine [1]. Traditionally, PI is commercially prepared by the phosgenation of aniline. The phosgenation process suffers from the difficulty of handling toxic phosgene as well as from the highly corrosive by-product HCl. To minimize the environmental impact of phosgene, green routes without the phosgenation step have been extensively studied [2–4]. Among them, the Scheme 1 represents an attractive synthesis route to PI. This method involves two steps: the catalytic production of methyl *N*-phenyl carbamate (MPC) by the methoxycarbonylation from aniline and dimethyl carbonate (DMC) (Eq. 1) [5–7] and decomposition of MPC (Eq. 2). This route has a number of advantages: (i) environmentally benign character of reactant (DMC), (ii) high selectivity of the process, and (iii) the by-product methanol can be recycled for the DMC synthesis [8, 9].

Up to now, the key step has been the catalytic decomposition of MPC, which is a reversible reaction in which PI may recombine with methanol. The interception of methanol to prevent this recombination has been accomplished by using boron halides in the presence of triethylamine [10, 11]. Despite the effectiveness of this method, it may not succeed commercially on a large scale because it is difficult to recycle the stoichiometric amounts of boron derivatives and triethylamine. On the other hand, various catalysts have been studied for the catalytic decomposition of MPC. Spohn [12] proposed a homogeneous dibutyltin

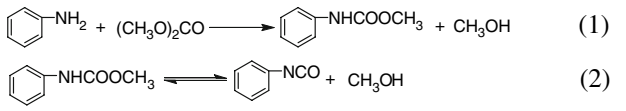

Scheme 1 Phosgene-free synthesis route to PI

dimethoxylate catalyst for the catalytic decomposition of MPC. The conversion and selectivity for MPC and PI were 33% and 99%, respectively, using the toluene as solvent and a reaction period of 40 min at temperature of 360 K. Though there was a high selectivity for that catalyst, the difficulty of re-use impedes its industrialization. Uriz [13] performed the catalytic decomposition of MPC using montmorillonite K-10 as the catalyst. The reaction was conducted for a period of 5 h at a temperature of 456 K under the conditions of MPC/montmorillonite K-10 = 0.6 mmol/100 mg and 8 mL *o*-dichlorobenzene (ODCB) as solvent. The experimental results showed that the conversion of MPC was high to 96%, however, the yield for PI was not reported. Furthermore, the efficiency is low because the amount of catalyst was relatively large (the mass of montmorillonite K-10/ MPC = 0.9) and a long reaction time (5 h) was required. Consequently, the development of more efficient catalysts is desirable.

Bismuth oxides are attractive catalysts for their high oxide-ion conductivity properties, and for their wide use for industrial selective oxidation reactions, especially for the propylene selective oxidation to acrolein and propylene ammoxidation to acrylonitrile [14, 15]. Such catalytic properties have been attributed to the existence of two different oxidation states of Bi (III and IV) and to the high mobility of lattice oxygen [16]. The surface reactivity of this oxide system is associated with the presence of defects. For instance, the existence of surface oxide ions with defective coordination numbers induces the extraction of an α-hydrogen from alkenes [17]. At the same time, it was reported that the decomposition reaction of carbamates followed an E1cB mechanism [18], in which the hydrogen was firstly removed from the N–H group of the carbamate. Therefore, the bismuth oxide was supposed to be active in the catalytic decomposition of MPC. In this paper, bismuth oxide catalysts have been prepared and characterized. Their catalytic property was investigated in the decomposition of MPC and then the reaction condition was optimized.

2 Experimental

2.1 Chemical Reagent

ODCB, MgO, CaO, PbO, Pb_3O_4, Sb_2O_3, Bi_2O_3, V_2O_5, Nb_2O_5, CrO_3, MoO_3, Fe_2O_3, ZnO, TiO_2, La_2O_3 were obtained from local manufactures and were of laboratory reagent grade. Several chemical reagents with AR grade were used for preparation of the catalyst, e.g., $Bi(NO_3)_3 \cdot 5H_2O$, $NH_3 \cdot H_2O$, NaOH. MPC (>99%) was self-prepared in the laboratory.

2.2 Catalyst Preparation

Catalysts were prepared from bismuth (III) nitrate pentahydrate by four methods: direct decomposition (B-1), mechano-chemical (B-2), direct precipitation (B-3), and indirect precipitation (B-4).

Catalyst B-1: Bi_2O_3 was prepared by the calcination of bismuth nitrate pentahydrate at 723 K in air for 4 h.

Catalyst B-2 [19]: Bi_2O_3 was prepared by mixing bismuth nitrate pentahydrate and NaOH in a mortar in 1:3 molar ratio. The mixture was milled for 0.5 h. The yellow solids were washed with alcohol and deionized water 3 times, respectively. Then the solids were dried at 353 K for 6 h in a vacuum drier.

Catalyst B-3 [20]: 40 mL 0.6 mol L^{-1} $Bi(NO_3)_3$ aqueous solution was quickly poured into the 30 wt.% NaOH solution. After constant stirring at 363 K for 2 h, the obtained yellowish precipitates were filtered and washed with alcohol and deionized water 3 times, respectively. Then the solids were dried at 353 K for 6 h in a vacuum drier.

Catalyst B-4: Bi_2O_3 was prepared by constantly dropping a 1.26 mol L^{-1} aqueous ammonia solution into a 150 g L^{-1} $Bi(NO_3)_3$ solution. After constant stirring at 333 K for 2 h, the precipitates were filtered and washed with alcohol and deionized water 3 times, respectively. The white solids were first dried at 393 K for 2 h, and then calcined at 723 K in air for 4 h.

2.3 Catalyst Characterizations

The structure and phase composition of the catalysts were determined by a Philip X'Pert Pro MPD X-ray diffraction between 25° and 60° (2θ) with a scanning rate of 0.1°/s, employing Cu Kα radiation ($\lambda = 1.54056$ Å), operated at 50.0 kV and 35.0 mA.

BET specific surface area and the total pore volume of the samples were measured by the nitrogen adsorption at 77 K on a Quantachrome NOVA 1000e apparatus. The surface area was calculated by using the conventional Brunauer–Emett–Teller (BET) method. The total pore volume was calculated from the amount of nitrogen absorbed at a relative pressure (P/P_0) close to unity.

The nature of the surface groups was determined by Fourier transform infrared spectroscopy (FT-IR). The FT-

IR spectra were collected by using a Nicolet 560 spectrometer in KBr pellets. The samples were mixed with KBr, and exposed to infrared light. The pellets were immediately measured after preparation under ambient conditions in the mid-infrared area. The spectra were the averaging results of 32 scans for each sample in wavelength ranging from 4000 to 400 cm^{-1}.

Microstructure characterization was carried out using a JEM-1000CX transmission electron microscope (TEM), operated at 80 kV. The samples were firstly dispersed by ultrasonic treatment, and then placed onto copper grids covered with holey carbon film.

The surface electronic structure of the catalysts was determined by X-ray photoelectron spectroscopy (XPS). The XPS spectra were acquired at room temperature with a Kratos Model XMSA 800 instrument using a monochromatic radiation source focused at (12 kV × 15 mA) Mg Kα (1253.6 eV). The residual pressure in the spectrometer chamber was 2×10^{-6} Pa during data acquisition. The spectrometer was calibrated by assuming the binding energy (BE) of the Au 4f (84.0 eV) and Ag 3d (386.3 eV) with respect to the Fermi level.

2.4 Catalytic Performance Testing and Reaction Procedure

The reaction was carried out in a 100 mL three-neck round-bottomed flask, equipped with a magnetic stirring bar, a nitrogen inlet with a thermometer, and a distillation apparatus. The ODCB was utilized as the solvent. The MPC, ODCB solvent and the catalyst were charged into the flask under atmospheric pressure. The mixture was quickly heated to react at 449–451 K, the boiling point of ODCB at the local atmospheric pressure. During the reaction, the methanol was continuously removed from the reaction system. After the reaction, the mixture was immediately derived by means of di-*n*-butylamine for analysis. The catalyst was filtered, and the filtrate was analyzed by high pressure liquid chromatograph (HPLC).

2.5 Product Analysis

Waters-515 HPLC was utilized for analyzing the reaction liquid. The analytical conditions were as follows: the model of the chromatographic column was Waters Symmetry Shield RP18 (Φ3.9 mm × 150 mm); the temperature of the chromatographic column was 313 K; the flow rate was 0.95 mL/min. CH_3OH/H_2O (60/35, v/v) was used for the mobile phase; the UV detection was Waters 2487; and the wavelength for detection was 260 nm. HPLC-MS was used to analyze qualitatively byproducts of the reaction. The mass spectrometer was used in ESI code at 523 K. The acquisition was performed from 50 to 400 amu (*m/z*).

3 Results and Discussion

3.1 Qualitative Analysis of Byproducts During the Synthesis of PI

In the synthesis of PI using the catalytic decomposition of MPC, there were several byproducts. The HPLC was applied to the analysis of the reaction products (ODCB was the solvent for reaction). The results were illustrated in Fig. 1. Two by-products were found, one of them was *N*,*N*′-diphenylurea (DPU), another was diphenylcarbodiimide (DPCD). The results were in agreement with the results of [21], and one side reaction was as follows (Eq. 3)

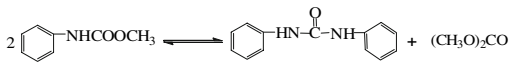

(3)

In the beginning, the byproduct at 15.0 min retention time could not be precisely identified, the dimmer of PI (uretidinedione) [22] or DPCD [23] could be the potential byproduct. In order to identify this unknown byproduct, the reaction liquid was analyzed by HPLC-MS. According to the result of HPLC-MS analysis, the unknown product was DPCD, and the main ion peaks of characteristic fragment (*m/z*) were 92.2, 117.1, 119.2, 121.2, 149.3, 168.4, and 195.3. In our experiments, it was found that the further reaction of PI could lead to the production of DPCD, so this side reaction was described as follows (Eq. 4):

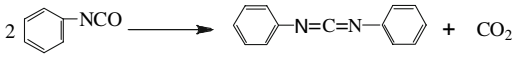

(4)

In summary, the reaction system was described as follows (Scheme 2):

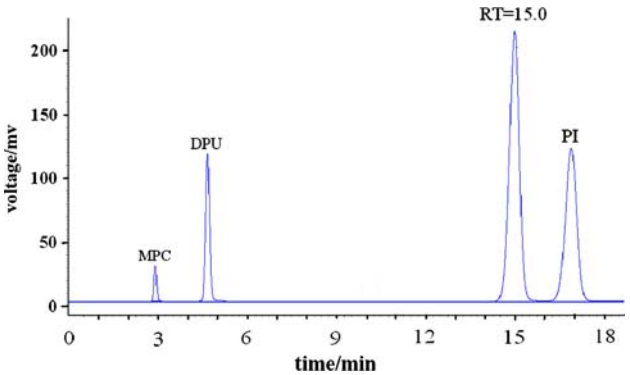

Fig. 1 HPLC result of products of MPC catalytic decomposition

3.2 The Catalytic Performance of Metal Oxide Catalyst

Metal oxides as heterogeneous catalysts for the catalytic decomposition of MPC had been seldom reported previously. The results of catalytic performances of various oxide catalysts for this reaction were demonstrated in Table 1.

As shown in Table 1, in the blank test with absence of catalyst, the conversion of MPC was only 19.5% with an excellent selectivity of PI (96.3%). For the *d*-block metal oxides, they didn't give high activity. The activity for catalytic decomposition of MPC had the order: $La_2O_3 > TiO_2$, $Fe_2O_3 > ZnO > MoO_3$, $V_2O_5 > CrO_3$, Nb_2O_5. The CrO_3 and Nb_2O_5 samples were essentially inactive for this reaction. It was notable that the heavy *p*-block metal oxides had the higher activity. Especially, PbO had the better activity (93.6% conversion). However, its activity was so strong that many byproducts accompanied with PI. This effect decreased the selectivity and yield of PI desired product. Moreover, Pb compounds are not friendly to environment. Sb^{3+}, Pb^{2+} and Bi^{3+} ions owned a $5s^2$ or $6S^2$ outermost orbital, there was a high cation polarizability for each of them, and the order of cation polarizability was $Pb^{2+} > Bi^{3+} > Sb^{3+}$ [24]. It seemed that the high polarizability of Pb^{2+} and Bi^{3+} supported the extraction of hydrogen from the N–H group and improved the catalytic activity of their metal oxides.

The specific surface areas and pore properties of five typical oxides were measured by nitrogen adsorption and desorption experiments. The nitrogen adsorption–desorption isotherms were illustrated in Fig. 2. The isotherms of La_2O_3, Nb_2O_5, Sb_2O_3 and Bi_2O_3 could be classified as a typical type Langmuir III according to the IUPAC classification. However, the isotherm of PbO was not of the typical Langmuir type. At the initial low pressure for PbO sample, the adsorbed volume decreased while the pressure increased. Among above metal oxides, the specific surface area of PbO (0.392 m^2/g) was the smallest. Thus, the specific surface area was not the key factor for the activity variation of these metal oxides.

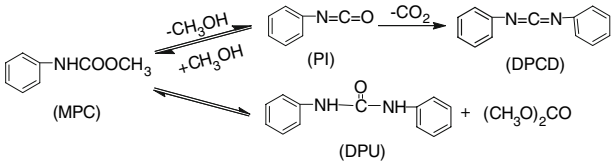

Scheme 2 Catalytic reaction system of MPC decomposition catalyzed by Bi_2O_3

For other samples, their catalytic results were also analyzed. The MgO and CaO manifested a medium activity for the catalytic decomposition of MPC. Furthermore, The activity of MgO was better than that of CaO. It seemed that the strong basicity was not helpful for the catalytic decomposition of MPC. On the other hand, the selectivity of DPU on acid α-Al_2O_3 was the highest. This indicated that the strong acidity promoted the DPU side reaction (Eq. 3). Busca [25] proposed that the acidity and basicity of La_2O_3, Sb_2O_3 and Bi_2O_3 were medium-weak Lewis acid and medium-strong base. Thus, the catalytic decomposition of MPC to PI product should be occurred at a proper acid–base strength. The MPC catalytic decomposition was a reaction with acid–base synergic effect.

In brief, the Bi_2O_3 catalyst gave the better catalytic performance. The catalytic performances of several Bi_2O_3 samples on the catalytic decomposition of MPC were discussed in detail in the following section.

3.3 Impact of Preparation Conditions on Activity and Selectivity of Bi_2O_3 Catalyst

3.3.1 Catalytic Activity of Bi_2O_3 Prepared by Different Methods

Chemical, micro-structural and catalytic properties of Bi_2O_3 catalysts depend on the synthesis procedure. Gotić

Table 1 Catalytic activity of different metal oxides

Blocks	Catalyst	Conversion of MPC (%)	Selectivity (%)		Blocks	Catalyst	Conversion of MPC (%)	Selectivity (%)	
			PI	DPU				PI	DPU
–	–	19.5	96.3	2.4	*s*	MgO	47.0	76.3	6.7
d	Nb_2O_5	13.4	87.1	3.7		CaO	38.4	71.5	5.7
	CrO_3	19.4	82.4	3.1	*p*	SiO_2	38.5	86.5	1.2
	V_2O_5	26.7	76.0	3.2		α-Al_2O_3 (acid)	43.3	81.6	13.5
	MoO_3	39.7	87.4	1.6		α-Al_2O_3 (basic)	54.3	45.7	5.8
	ZnO	44.1	80.6	3.2		PbO	93.6	52.8	6.2
	TiO_2	46.0	73.0	2.1		Pb_3O_4	83.7	70.4	7.5
	Fe_2O_3	45.9	92.5	2.6		Bi_2O_3	75.1	92.6	2.8
	La_2O_3	48.6	94.6	3.1		Sb_2O_3	49.6	92.6	3.2

The metal oxides were pretreated at 473 K for 2 h. MPC: methyl *N*-phenyl carbamate, PI: phenyl isocyanate, DPU: *N*,*N*′-diphenylurea. Reaction conditions: reaction temperature: 449–451 K, MPC: 0.02 mol, m(ODCB)/m(MPC) = 15, m(catalyst)/m(MPC) = 0.05, reaction time: 1 h

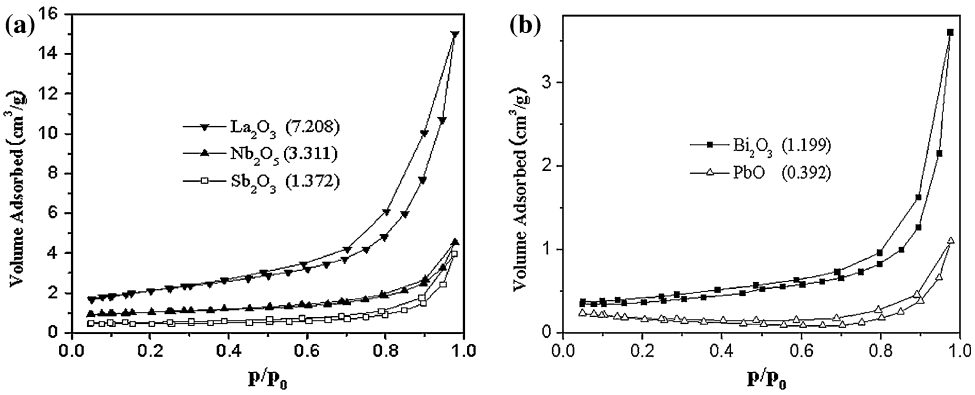

Fig. 2 Nitrogen adsorption–desorption isotherm patterns and the specific surface area (m^2/g)

[26] investigated the morphology of Bi_2O_3 particles prepared by a modified sol–gel procedure. Irmawati [27] investigated the influence of bismuth content on the surface area and crystal size of Bi_2O_3 nanocrystals via precipitation method. In this paper, several Bi_2O_3 catalysts from bismuth nitrate pentahydrate were prepared by different synthesis routes. The structures of these Bi_2O_3 catalysts by different preparation methods were characterized by XRD. The results were shown in Fig. 3.

The Bi_2O_3 system has six different polymorphs with different structures and properties, labeled α-, β-, γ-, δ-, ε-, and ω-phases [28]. The phase of catalyst B-3 is mainly the α-Bi_2O_3 (PDF card No. 41-1449), which is as same as the phase of the commercial sample. The XRD patterns recorded for B-1, B-2 and B-4 samples corresponded to a mixture of monoclinic α-Bi_2O_3 and tetragonal β-Bi_2O_3 (PDF card No. 27-0050) [26]. The main peaks of α-Bi_2O_3 appeared at $2\theta = 27.4°(120)$, $33.3°(200)$, $46.3°(041)$, and those of β-Bi_2O_3 appeared at $2\theta = 27.9°(201)$, $32.7°(220)$, $46.2°(222)$, $55.5°(421)$. In addition, due to incomplete reaction, catalyst B-1 and B-2 contained small amount of crystalline of $Bi_5O_7NO_3$ (PDF 51-0525).

The FT-IR analyses were performed in the 4000–400 cm^{-1} frequency range on Bi_2O_3 powders. FT-IR spectra of the catalysts prepared by different methods are shown in Fig. 4. The spectra displayed a broad absorption band in the 546–434 cm^{-1} range. This is due to the Bi–O stretching mode. This phenomenon is in agreement with data reported by Carrazan [29], in which it was indicated that in the 600.00–400.00 cm^{-1} range, the stretching and deformation modes involving Bi–O modes are expected. The absorption band at 1384 cm^{-1} and 3455 cm^{-1} were assigned to the vibrations of NO_3^- and OH^-, respectively. Furthermore, the intensity of hydroxyl groups has the order: B-2 > B-1 > B-3. There were hydroxyl groups on the surface of metal

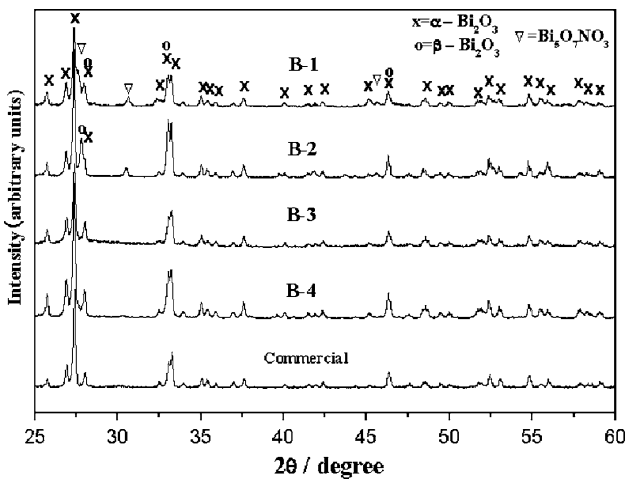

Fig. 3 XRD patterns of Bi_2O_3 samples prepared by different preparation methods

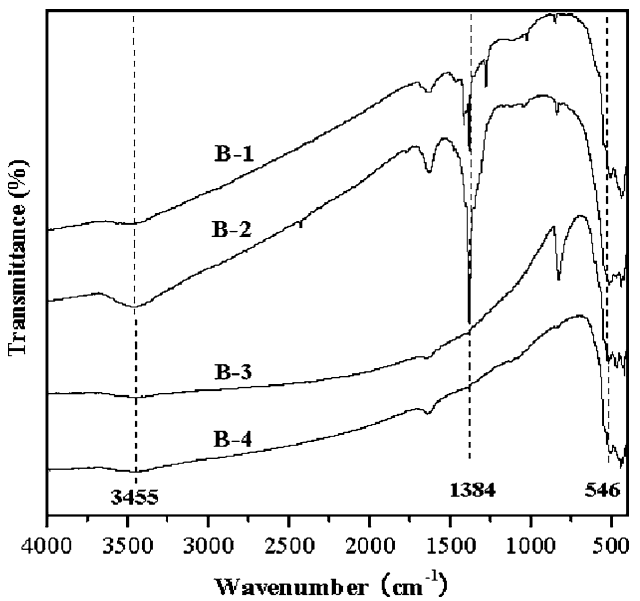

Fig. 4 FTIR of Bi_2O_3 samples prepared by different preparation methods

oxide, due to the dissociative adsorption of water. One of the reasons for the difference of OH^- concentration on Bi_2O_3 samples was the difference of the surface area (see Table 2).

The catalytic performances of Bi_2O_3 samples prepared by different methods were investigated. The results are shown in Table 2. Catalyst B-3 had almost the same activity as commercial Bi_2O_3 (see Table 1), this could be ascribed to the fact that both of their phase is mainly the α-Bi_2O_3. On the other hand, with some of β-Bi_2O_3 phase, Bi_2O_3 samples prepared by other methods showed higher activity than commercial Bi_2O_3. Among them, catalyst B-2 had the highest activity; however, its selectivity for PI was somewhat low (see Table 2). The larger surface area of catalyst B-2 was attributed to its highest catalytic activity. At the same time, as more NO_3^- groups appears on the surface of B-2, more DPCD are formed (see Scheme 2), which leads to the decrease of PI selectivity. In general, the catalyst B-1 had a better catalytic performance for the MPC decomposition. Thus, the preparation parameters in the direct thermal treatment of bismuth nitrate pentahydrate were investigated in detail in the next paragraph for a better performance.

3.3.2 *Role of Thermal Treatment on the Activity and Selectivity of Bi_2O_3 Catalyst*

The activity of catalysts calcined at different temperature are shown in Fig. 5a. For the catalyst calcined at 673 K, though the catalyst possessed moderate activity, its selectivity to PI was somewhat lower due to the formation of more DPCD. As the calcination temperature was increased to 723 K, there was a significant activity and an optimal selectivity to PI. The activity of the catalysts increased slightly as the calcination temperature was further increased to 773 K. Thereafter it decreased. In addition, the calcination temperature had little relationship with the DPU selectivity of the catalyst, which remained almost constant as the calcination temperature increased. Thus, the best catalytic performance of the Bi_2O_3 catalyst appeared at the calcination temperature of 723–773 K.

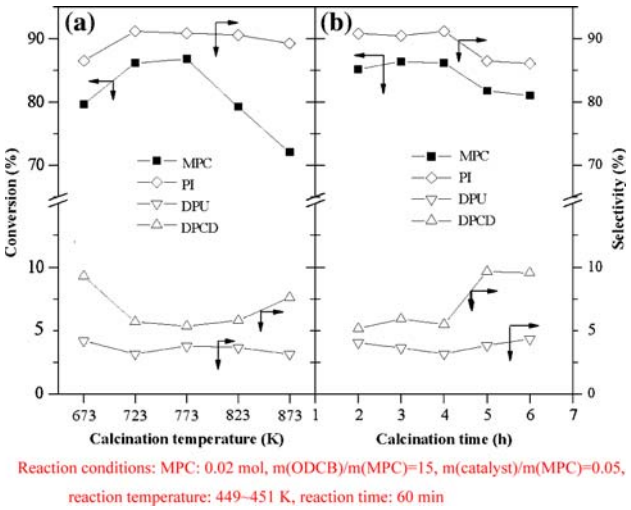

Fig. 5 Effect of thermal treatment on the catalytic performance

For the catalyst calcined at 673 K, the color of catalyst is mainly white and the yellow-colored character of Bi_2O_3 is not obvious. It can be seen that most of Bi_2O_3 phase isn't formed at 673 K. The TEM micrographs of the Bi_2O_3 particles at different calcination temperatures are shown in Fig. 6. From TEM images in Fig. 6, the catalyst calcined at 723 K contains α-Bi_2O_3, consisting of particles of varying shapes and sizes and well-dispersed plate-like β-Bi_2O_3 [26], which is in agreement with the XRD results discussed earlier (Fig. 3). After calcination at higher temperature above 773 K, serious agglomeration of Bi_2O_3 took place and the Bi_2O_3 particles became large (Fig. 6).

The catalytic behavior of another five catalysts with different calcination time is shown in Fig. 5b. The results are similar with those of calcination temperature. The Bi_2O_3 catalyst calcined for 2 h possessed comparable activity. Thereafter, the activity increased slightly. The best catalytic performance appeared at the calcination time of 4 h. As the calcination time of these catalysts was further increased, there was a decrease in activity and the selectivity of PI. The selectivity towards DPU also changed slightly with the increased calcination time. In general, the optimal calcination time for the Bi_2O_3 catalysts was 3–4 h.

Table 2 Properties and catalytic performances of Bi_2O_3 samples prepared by different methods

Catalyst	Specific surface area (m^2/g)	Specific pore volume ($\times 10^{-3}$ cm^3/g)	MPC conversion (%)	Selectivity (%)		
				PI	DPU	DPCD[a]
B-1	1.003	5.192	86.2	91.2	3.2	5.7
B-2	3.096	13.020	89.6	82.1	5.9	12.0
B-3	0.613	1.688	74.7	92.5	2.5	5.0
B-4	–	–	81.3	92.1	2.9	5.1

[a] Sel.(DPCD) = 1-Sel.(PI)-Sel.(DPU). MPC: methyl *N*-phenyl carbamate, PI: phenyl isocyanate, DPU: *N*,*N*′-diphenylurea, DPCD: diphenylcarbodiimide. Reaction conditions: MPC: 0.02 mol, *m*(ODCB)/*m*(MPC) = 15, *m*(catalyst)/*m*(MPC) = 0.05, reaction temperature: 449–451 K, reaction time: 60 min

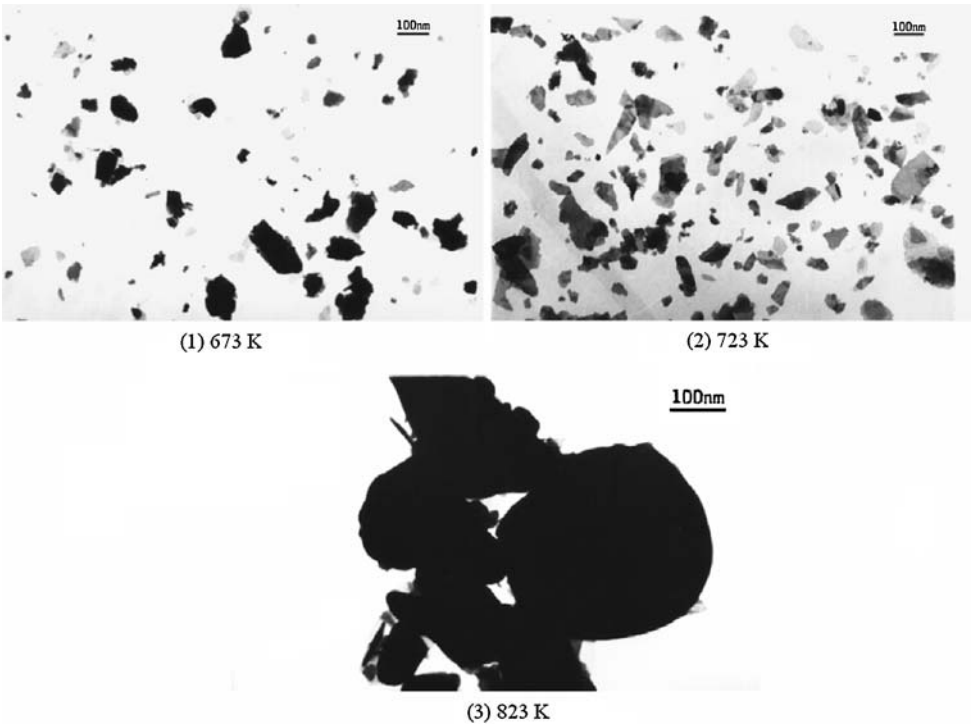

Fig. 6 TEM micrographs of the Bi_2O_3 particles at different calcination temperatures

3.4 Effects of Reaction Conditions on the Activity and Selectivity of Bi_2O_3 Catalyst

3.4.1 Impact of Catalyst Amount

The impact of the catalyst amount on the catalyst performance was examined at m(ODCB)/m(MPC) = 15. As shown in Fig. 7a, the MPC conversion increased rapidly when the mass ratio of the catalyst B-1 to MPC was increasing below 0.05. When the mass ratio of the catalyst B-1 to MPC was above 0.05, the MPC conversion increased slightly. A high selectivity of PI (94.2%) could be obtained with a low catalyst amount (the ratio was 0.02), whereas the selectivity of PI decreased slightly as the mass ratio of catalyst B-1 to MPC increased. This might be ascribed to the fact that more amount of catalyst would be also in favor of the side reaction (see Scheme 2): equilibrium shifting to DPU synthesis. As a result, the selectivity of DPU increased with the increase of the catalyst amount. Based on the results of MPC conversion and PI selectivity, the optimal mass ratio of the catalyst B-1 to MPC was 0.05.

3.4.2 Influence of MPC Concentration

The impact of MPC concentration on the catalytic performance and product selectivity was examined by changing the amount of ODCB solvent. As shown in Fig. 7b, the MPC conversion increased with the increase of MPC concentration. This was attributed to the more opportunity for contact between the catalysts with MPC. In addition, the selectivity of PI declined with the increase of MPC concentration. This was caused by the disproportion of MPC together with the carbonization of PI (see Scheme 2) at a high concentration, especially above the concentration of 8 wt.%. Based on the results of MPC conversion and selectivity of PI, the optimal initial MPC concentration was 6–7 wt.%.

3.4.3 Role of Reaction Time

The catalytic decomposition of MPC was also monitored by changing the reaction time. As shown in Fig. 7c, the MPC conversion increased sharply within 45 min. After 60 min of reaction, the conversion of MPC increased slightly with the prolonged reaction time. It could be seen that the catalytic decomposition of MPC by catalyst B-1 was a fast equilibrium reaction. In addition, the selectivity of DPU had little relationship with the reaction time while the selectivity of PI decreased with the reaction time. The longer was the PI stay in the reaction system, the more DPCD by-product was formed via the carbonization of PI. Based on the results of MPC conversion and PI selectivity, the optimal batch reaction time was 60 min.

From above studies and observations, the optimal reaction conditions over Bi_2O_3 catalyst B-1 were as follows: catalyst/MPC ratio = 0.05 (mass), ODCB/MPC = 15

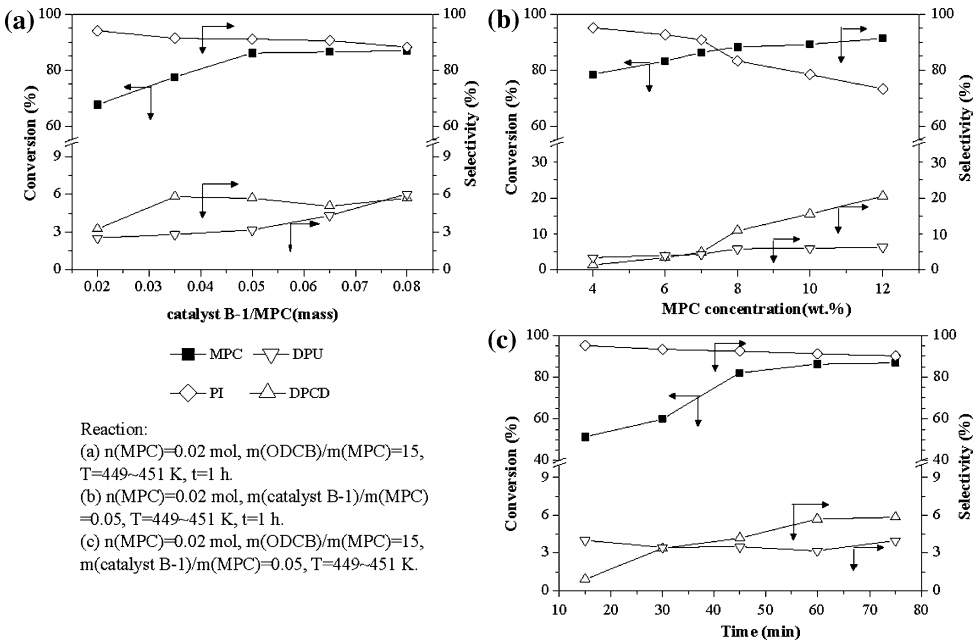

Fig. 7 Effect of reaction condition on the catalytic performance: (**a**) catalyst amount, (**b**) MPC concentration, and (**c**) reaction time

(mass), batch reaction time of 60 min. The obtained MPC conversion was 86.2%, and the highest yield of PI was 78.5%.

3.5 Durability of Bi_2O_3 Catalyst

In order to study the stability and re-usability of the Bi_2O_3 catalyst, the recovered catalyst B-1 was washed by acetone and distilled water, then dried at 393 K and used again under the same conditions. As shown in Fig. 8, unconventionally, the activity and PI selectivity of the catalyst B-1 used once manifested a slight increase. This might be ascribed to some changes with the chemical environment of the Bi_2O_3. It can be seen from Fig. 9 that a new crystalline phase of Bi_2O_4 (PDF 50-0864) appeared when catalyst was used once. This showed that the Bi (+3) centers of the catalyst B-1 had partially been oxidized to Bi (+4) centers. When the re-use times further increased, the peak at 29.5° and 30.0° (2θ) of Bi_2O_4 phase became more obvious, however, most of the diffraction peaks of Bi_2O_3 could not be observed when catalyst was used four times. For the results of catalyst activity and product selectivity, they decreased only slightly when it was re-utilized for four times.

The surface property of the fresh catalyst B-1 and that of used sample were investigated by XPS. The results are shown in Fig. 10. The major peaks around 158.7 and 164.1 eV correspond to Bi $4f_{7/2}$ and Bi $4f_{5/2}$, respectively. These binding energy values are those of Bi with an oxidation state of 3+ [30]. It can be observed from Fig. 10(1)

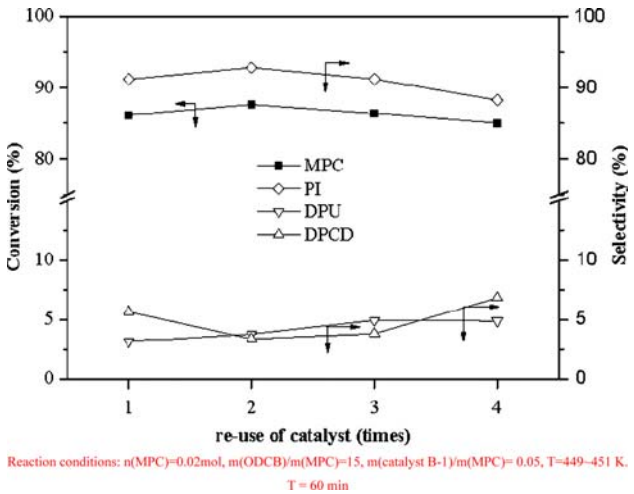

Fig. 8 Influence of re-use of Bi_2O_3 catalyst on performance

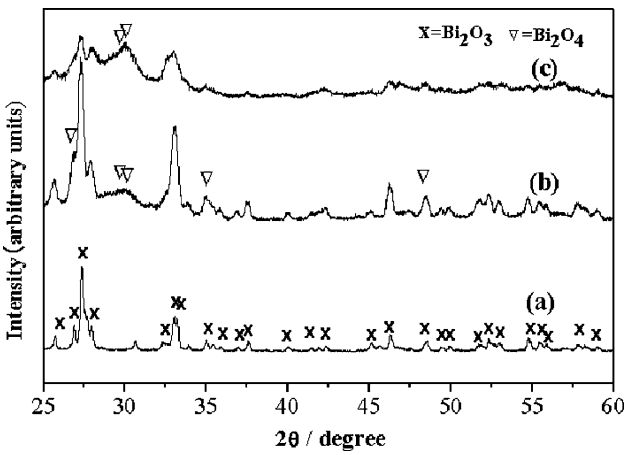

Fig. 9 X-ray diffraction patterns of fresh and used catalysts: (a) fresh catalyst, (b) used once, and (c) used fourth time

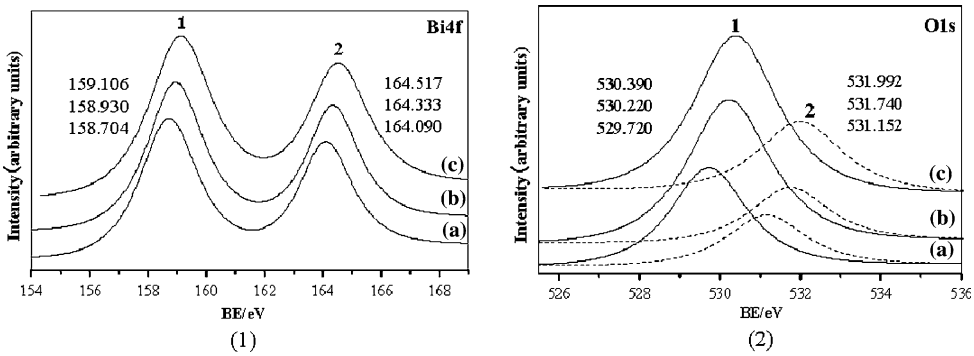

Fig. 10 XPS spectra of Bi 4f and O1s of the Bi_2O_3 catalysts at different stages: (a) fresh sample, (b) used once, and (c) used fourth times

that binding energy shifted to a higher value for Bi $4f_{7/2}$ and Bi $4f_{5/2}$ as the usage time increased. This indicated that the Bi (+3) centers were partial oxidized from Bi(III) to Bi(IV) [30, 31] during the reaction process, which is in agreement with the XRD analysis. The O1s peak of Fig. 10(2), which shows a marked broadening towards higher BEs, contains two components: the first, at 529.7 eV, is due to O_2^- of the bismuth oxide; and the second, at 531.1 eV, is attributable to the OH^- group adsorbed on the surface [30], in accordance with the results of the FT-IR analysis. In accordance with Dimitrov [24], the increase of metal binding energy in XPS spectra of simple oxides was accompanied by an increase of O1s binding energy. The O1s peak in the XPS spectra shifted also to higher binding energy.

4 Conclusions

Upon comparing the catalytic performance of various metal oxides, the metal oxides which have medium acid–base strength gave higher catalytic activity. The catalytic performances of Bi_2O_3 catalysts for the decomposition of MPC were investigated in this work.

HPLC-MS results show that the formation of DPU and that of DPCD are the main competitive reactions in the PI synthesis. The strong acidity promoted the DPU side reaction. The reaction conditions catalyzed by Bi_2O_3 sample were optimized: mass ratio of ODCB to MPC of 15:1, the catalyst amount of 5.0% (mass ratio to MPC), and a reaction time of 60 min. The conversion of MPC was 86.2%, and the yield of PI was 78.5%.

From the characterization results, Type of Bi_2O_3 phase and surface area are the important for Bi_2O_3 catalyst. The Bi_2O_3 catalyst contained more β-Bi_2O_3 phase and larger surface area had a higher catalytic activity. The existence of NO_3^- on the surface of catalyst resulted in more DPCD by-product formed. There was a better catalytic performance for the Bi_2O_3 catalyst prepared by the direct calcination of bismuth (III) nitrate pentahydrate at 723 K for 4 h in air. The surface Bi (III) ions were partially oxidized to Bi (IV) ions during reaction, which enabled a little increase in catalytic activity. In brief, an effective heterogenous catalyst Bi_2O_3 was developed and investigated in detail for friendly preparation of isocyanates by the catalytic decomposition of carbamates.

Acknowledgments This work was supported by the National High Technology Research and Development Program of China with project number 2006BAC02A08.

References

1. Chadwick DH, Cleveland TH (1981) In: Grayson M (ed) Encyclopedia of chemical technology, 3rd edn. Wiley, New York, p 793
2. Ragaini F, Cenini S (1996) J Mol Catal A 109:1
3. Srivastava R, Manju MD, Srinivas D, Ratnasamy P (2004) Catal Lett 97:41
4. Ono Y (1997) Appl Catal A: Gen 155:133
5. Fu ZH, Ono Y (1994) J Mol Catal A 91:399
6. Katada N, Fujinaga H, Nakamura Y, Okumura K, Nishigaki K, Niwa M (2002) Catal Lett 80:47
7. Li F, Miao J, Wang Y, Zhao X (2006) Ind Eng Chem Res 45:4892
8. Cai Q, Jin C, Lu B, Tangbo H, Shan Y (2005) Catal Lett 103:225
9. Drake IJ, Fujdala KL, Bell AT, Don Tilley T (2005) J Catal 230:14
10. Valli VLK, Alper H (1995) J Org Chem 60:257
11. Butler DCD, Alper H (1998) Chem Commun 23:2575
12. Spohn RJ (1984) US patent 4487713
13. Uriz P, Serra M, Castillon S, Salagre P, Claver C, Fernandez E (2002) Tetrahedron Lett 43:1673
14. Arora N, Deo G, Wachs IE, Hirt AM (1996) J Catal 159:1
15. Hanna TA (2004) Coord Chem Rev 248:429
16. Iwamoto M, Yoda Y, Yamazoe N, Seiyama T (1978) J Phys Chem 82:2564
17. Driscoll DJ, Martir W, Lunsford JH (1987) J Phys Chem 91:3585
18. Bergon M, Ben Hamida N, Calmon JP (1985) J Agric Food Chem 33:577
19. Li Q, Li J, Xia X, Cao Y (1999) Acta Chim Sinica 57:491
20. Li W (2006) Mater Chem Phys 99:174
21. Wang Y, Zhao X, Li F, Zhang W, Hao D (1999) Acta Petrol Sin (Pet Process Sect) 15:9
22. Duong HA, Cross MJ, Louie J (2004) Org Lett 6:4679
23. Yoshitake N, Furukawa M (1995) J Anal Appl Pyrolysis 33:269
24. Dimitrov V, Komatsu T (2002) J Solid State Chem 163:100

25. Busca G (1999) Phys Chem Chem Phys 1:723
26. Gotić M, Popović S, Musić S (2007) Mater Lett 61:709
27. Irmawati R, Noorfarizan Nasriah MN, Taufiq-Yap YH, Abdul Hamid SB (2004) Catal Today 93–95:701
28. Drache M, Roussel P, Wignacourt JP (2007) Chem Rev 107:80
29. Carrazan SRG, Martin C, Rives V, Vidal R (1996) Spectrochim Acta Part A 52:1107
30. Barreca D, Morazzoni F, Rizzi GA, Scotti R, Tondello E (2001) Phys Chem Chem Phys 3:1743
31. Morgan WE, Van Wazer JR, Stec WJ (1973) Inorg Chem 12:953